ACS OMEGA

Open Access

http://pubs.acs.org/journal/acsodf

Article

Identification and Quantification of the Main Psychoactive Ingredients of Cannabis in Urine Using Excitation−Eemission Matrix Fluorescence Coupled with Parallel Factor Analysis

Sheng-Feng Cui,* Hai-Long Yang, Si-Yu Lin, Jing-Wei Wan, and Cheng-He Zhou

Cite This: *ACS Omega* 2023, 8, 36302−36310

Read Online

ACCESS | Metrics & More | Article Recommendations | Supporting Information

ABSTRACT: Cannabis is the most prevalent abused substance after alcohol, and its consumption severely harms human health and thus adversely impacts society. The identification and quantification of cannabis in urine play important roles in practical forensics. Excitation−emission matrix (EEM) fluorescence spectroscopy coupled with parallel factor (PARAFAC) analysis was developed to identify and quantify the four main ingredients of cannabis in urine samples. The main ingredients of cannabis including Δ-9-tetrahydrocannabinol (THC), cannabidiol, cannabinol, and tetrahydrocannabinolic acid (THC−COOH) exhibited diverse fluorescence characteristics, and the concentrations of these compounds depicted a positive linear relationship with the fluorescence intensity at the ng/mL level. The EEM/PARAFAC method adequately characterized and discriminated the four ingredients in calibration and prediction samples with a low root-mean-square error of prediction (RMSEP; 0.03−0.07 μg/mL) and limit of quantitation (LOQ; 0.26−0.71 μg/mL). The prediction results of the EEM/PARAFAC method well correlated with that of GC−MS with a low RMSEP range (0.01−0.05 μg/mL) and LOQ range (0.07−0.44 μg/mL) in urine samples. The EEM spectroscopic investigation coupled with the PARAFAC algorithm results in an organic, solvent-less, fast, reliable tool to perform accurate and rapid screening of cannabis abusers.

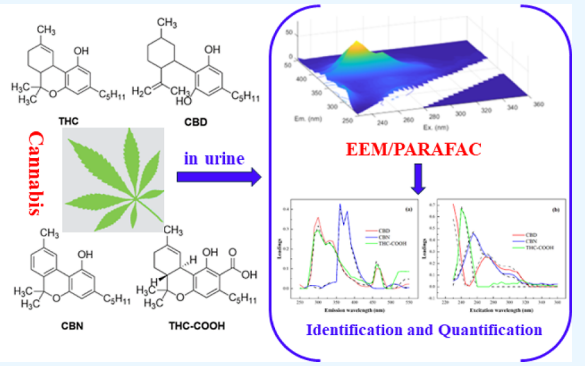

1. INTRODUCTION

With the recent trend regarding the legalization of cannabis, cannabis has become one of the most widely used recreational drugs.[1] The prevalence of cannabis use is considered a social threat, specifically for adolescents. Frequent cannabis users may cause cognitive deficits and psychomotor disorders. There is evidence that cannabis use is associated with an increased risk of motor vehicle crashes.[2] The cannabis plant (*C. sativa*) contains at least 140 cannabinoids. Δ-9-tetrahydrocannabinol (THC), cannabidiol (CBD), and cannabinol (CBN) are the main psychoactive ingredients of cannabis (Figure 1), which are particularly relevant for cannabis use.[3] THC and CBD engender markedly different pharmacological effects in humans and animals. THC exhibits reinforcing effects when examined under experimental conditions in primates or humans. Moreover, it can precipitate psychosis and compromise cognition and motor coordination in humans. The detection of cannabis in the field of forensic science focuses on the quantitative analysis of these three compounds.[4] THC−COOH as a biosynthetic precursor of THC and an intermediate product of the THC metabolism is another crucial detection target of cannabis in urine.[5]

Among the detection techniques of cannabis, chromatography is considered to be a powerful method for determining cannabis in biological samples (blood, urine, and hair) owing to its high accuracy, precision, and good sensitivity. However, it requires harmful organic solvents and large-scale expensive instruments, consumes a long time, and incurs high cost. More importantly, the use of organic solvents in this method is often accused of being unsustainable and not environmentally friendly.[6] The bulk detection of suspicious illegal cannabis samples in high-speed railway stations and streets is increasing gradually.[7] To support the extensive determination of cannabis, a rapid and simple method instead of an environmentally unfriendly and time-consuming chromatographic method is required to identify biological samples and seized illegal drugs.

Fluorescence spectroscopy with chemometric algorithms, e.g., excitation−emission matrix (EEM) and parallel factor (PARAFAC), is a nondestructive, high-speed, low-cost method with high selectivity.[8] There is no need for any complicated sample preparation before measuring the fluorescence of the

Received: July 9, 2023
Accepted: September 11, 2023
Published: September 21, 2023

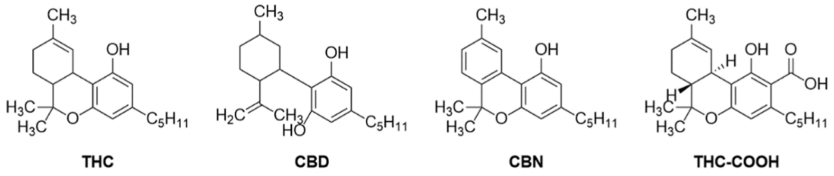

Figure 1. Chemical structures of THC, CBD, CBN, and THC−COOH.

sample, and the measured signal is 1000 times more sensitive than those generated by absorption-based spectrophotometric techniques. PARAFAC is a multiway method used for the resolution of trilinear data and can mathematically decompose the EEM complex fluorescence signal into individual fluorescence spectra via overlapping.[9]

PARAFAC applies a nonlinear optimization algorithm, namely, alternating least-squares, to analyze complex data systems considering constraints, e.g., non-negativity, which can be considered as one of the advantages of PARAFAC.[10] The uniqueness of PARAFAC solutions under mild conditions circumvents the rotational freedom problem. Thus, a PARAFAC model can handle large volumes of three-way data from fluorescent molecules regarding their relative concentrations and pure spectral profiles in the analyzed samples. EEM combined with the PARAFAC algorithm has been successfully implemented in various fields, e.g., dissolved organic matter in natural water, discrimination of photosystem II with/without water-oxidizing complex, natural organic matter in drinking water, and aromatic amino acids in plasma and urine.[11] Therefore, the EEM coupled with the PARAFAC algorithm can help determine cannabis in biological samples, which can create a new avenue for rapidly determining adulterated illegal drugs.

Considering the aforementioned discussion and as an extension of our previous study,[12−14] herein, the fluorescence signatures of the main psychoactive ingredients of cannabis were examined using the fluorescence-based EEM, and the linear regression parameters between fluorescence peak intensity and the ingredient concentration were studied as the basis of quantitative analysis. Moreover, the ability and further applications of this method to discriminate fluorescence signatures from the trace component were evaluated. Herein, the fluorescence-based EEM coupled with a parallel factor helped identify and quantify cannabis in urine.

2. MATERIALS AND METHODS

2.1. Chemicals and Instruments. With regard to the methods, 1.0 mg/mL standard THC, CBD, and CBN and 0.1 mg/mL THC−COOH were purchased from Cerilliant (Round Rock, TX, USA) for the methanol solution. The Milli-Q advantage ultrapure water system (Millipore, Germany), fluorescence spectrometer (F-4600 Hitachi, Japan) equipped with a xenon lamp (150 W), quartz cell (1.0 cm), and gas chromatography−mass spectrometry (GC−MS) (2010 PLUS, Shimadzu) with an HP-1 column (30 m × 0.25 mm × 0.33 mm) were used. Urine samples are divided into two groups: reference urine samples, which were collected from two nonconsumer volunteers and a certain amount of psychoactive ingredients were added, and other samples, which were donated by two anonymous frequent cannabis users.

2.2. Sample Preparation and Fluorescence EEM Analysis. The standard solutions of THC, CBD, CBN, and THC−COOH were used without further purification. All of the individual solutions with different concentrations were prepared by diluting the corresponding stock solution with methanol and ultrapure water, respectively. Calibration samples and prediction samples (three-component and four-component, respectively) were prepared by diluting the corresponding stock solution with methanol in the range from 60 to 960 ng/mL, respectively. Urine samples (10 mL) were collected from two nonconsumer and two consumer volunteers. Unspecified amounts of THC, CBD, CBN, and THC−COOH were added to the urine samples of nonconsumer volunteers, and the two types of urine samples were treated using the same preprocessing method; 2.0 mL of the urine sample was treated with 1.0 mL of sodium hydroxide solution (2.0 mol/mL) in a boiling water bath for 20 min. The mixture was cooled to room temperature and adjusted to a pH of 3.5 using 0.5 mL of hydrochloric acid solution (2.0 mol/mL) and 0.2 mL of acetic acid; then, it was further extracted with *n*-heptane (3.5 mL) for 20 min using an ultrasonic washer. Subsequently, the obtained mixture was centrifuged at 8000 rpm for 5 min, and the organic phase was obtained after centrifugation, extracted twice, and combined with the organic phase. The solvent was evaporated at 55 °C under reduced pressure. For the GC−MS method, the obtained solid was further treated with the derivatization reagent of *N*,*O*-bis(trimethylsilyl)trifluoroacetamide (80 μL) at 70 °C for 40 min, and then, the liquid supernatant was analyzed. However, the obtained solid was directly dissolved in methanol (0.2 mL) for the EEM/PARAFAC analysis.

2.3. Fluorescence EEM Analysis and GC−MS. The fluorescence EEM spectra were recorded using an F-4600 Hitachi luminescence spectrometer equipped with a quartz cell (1.0 × 1.0 × 4.5 cm); the widths of the excitation and emission slits were set as 5.0 nm, and increments of 5 nm were considered for EX and EM sampling intervals. The emission wavelength (λ_{em}) range was 250−550 nm, and the excitation wavelengths (λ_{ex}) ranged from 230 to 360 nm at a scan speed of 1200 nm/min.

Confirmatory analyses were performed using a Shimadzu GC−MS (2010 PLUS). A constant flow of helium at 1 mL/min was used as the carrier gas. The injection was segregated at a split ratio of 20:1. The oven temperature was set at 80 °C for 2 min and ramped to 280 °C at 30 °C/min; then, a postrun was performed at 280 °C for 10 min. The mass spectrometer parameters were set as follows: transfer line at 250 °C and ion source at 230 °C. Mass spectral data were collected in the scan mode at 40−450 *m*/*z*.

2.4. PARAFAC Modeling. For standard solutions and multicomponent solutions, the PARAFAC modeling of EEMs was conducted by using MATLAB 2010a with the N-way and DOM-Fluor toolboxes. The procedure was performed according to one of the reported studies.[15] The fluorescence EEM analysis helped generate a series of three-dimensional data matrices including emission wavelength, excitation wavelength, and fluorescence intensity data, which helped

https://doi.org/10.1021/acsomega.3c04913
ACS Omega 2023, 8, 36302−36310

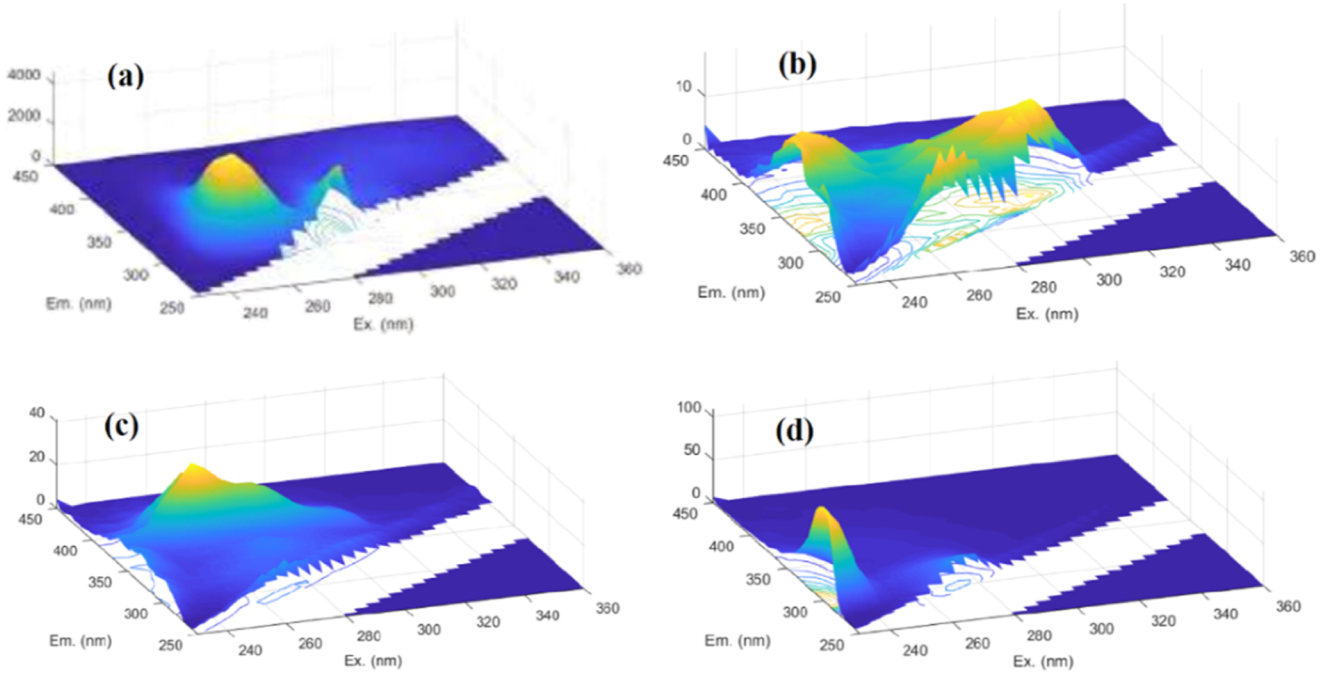

Figure 2. EEM of THC (a, 8 μg/mL), THC−COOH (b, 4 μg/mL), CBN (c, 1.56 μg/mL), and CBD (d, 2.1 μg/mL) after correcting for Raman scattering.

Table 1. Main Fluorescence Peaks of the Individual Psychoactive Ingredients of Cannabis in Methanol, and the Linear Regression Parameters between the Concentration and Fluorescence Peak Intensity are Also Presented[a]

compounds	$\lambda_{ex}/\lambda_{em}$ (nm)	Stokes shift (nm)	r^2	DL (ng/mL)	QL (ng/mL)	LR (μg/mL)
THC	255/310	55	0.998	1.8	6.0	0.05−1.5
CBD	235/300	65	0.999	0.9	2.9	0.06−0.9
THC−COOH	265/285	20	0.994	6.8	22.6	0.1−1.0
CBN	255/310	55	0.999	2.3	3.4	0.06−1.5
	310/360	40	0.998	4.2	7.9	

[a]Determination coefficient (r^2), detection limit (DL), quantification limit (QL), and linear range (LR) of the compounds were calculated from the equation of the linear regression between the contaminant concentration and the fluorescence peak intensity as following: DL = 3σ/a, QL = 10σ/a, where a is the slope and σ is the standard deviation of the y-intercept. σ values were calculated according to the formula: $\sigma = \sqrt{\frac{\sum(y_i - y_i')^2}{n-2}} \times \sqrt{\frac{\sum x_i^2}{n\sum(x_i - \bar{x})^2}}$, where n is the number of samples and x_i and y_i are the compound concentrations and the measured fluorescence intensities, respectively. yi' is the fluorescence intensities calculated from the linear regression equation, and x is the mean concentration.

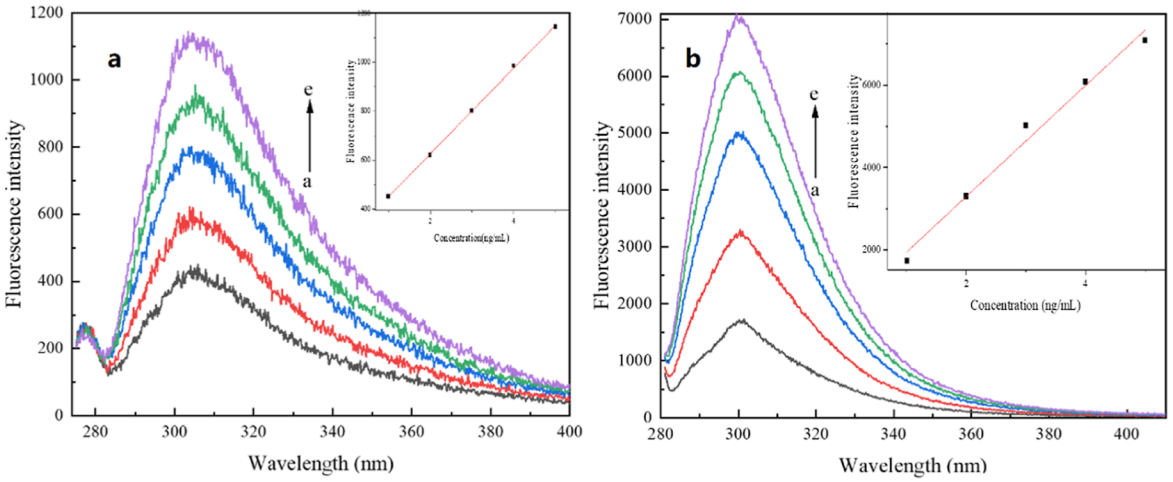

Figure 3. Fluorescence spectra of THC (a) and CBN (b) at different concentrations. Inset: the linear relationship between fluorescence emission peak intensity and concentration of THC (a) and CBN (b).

https://doi.org/10.1021/acsomega.3c04913
ACS Omega 2023, 8, 36302−36310

Table 2. Concentrations of Main Ingredients of Cannabis in the Simulated Mixtures (ng/mL)

	mixture 1 (ng/mL)				mixture 2 (ng/mL)				
samples	no	CBN	CBD	THC−COOH	no	CBN	CBD	THC−COOH	THC
calibration samples	1	60	60	100	9	60	60	100	60
	2	60	90	150	10	90	60	100	60
	3	90	150	200	11	90	150	200	60
	4	150	150	250	12	210	150	200	90
	5	180	210	250	13	270	210	300	150
	6	270	210	300	14	360	210	400	150
	7	300	270	300	15	360	330	400	210
	8	300	300	400	16	450	300	400	210
prediction samples	17	65	70	90	23	70	62	75	65
	18	85	90	120	24	88	95	140	85
	19	125	130	160	25	132	155	195	120
	20	340	320	330	26	325	305	340	210
	21	750	710	800	27	650	629	800	480
	22	950	900	950	28	980	920	1000	500

develop a data cube, i.e., X, for individual standards and multiple samples. PARAFAC helped derive a promising tool to examine the data matrices, which resulted in a three-way array of size $i \times j \times k$.

$$x_{ijk} = \sum_{n=1}^{N} a_{in} b_{jn} c_{kn} + e_{ijk}, \qquad i = 1, \cdots, I; \quad j = 1, \cdots, J; \; k = 1, \cdots, K \tag{1}$$

where x_{ijk} is the fluorescence intensity of the sample. J is the number of emission wavelengths, K is the number of excitation wavelengths, i is the number of samples, and N is the number of the components. a_{in}, b_{jn}, and c_{kn} are elements of A, B, and C matrices, respectively.

Raman and Rayleigh scattering in the solution were corrected according to the reported studies. In the calibration step, A scores were regressed against the real concentrations of each ingredient of cannabis in the mixtures to obtain a linear regression equation. In the prediction step, the obtained regression line was used to calculate the concentration of each compound in the prediction samples. The validation of the PARAFAC model and the determination of the correct number of components were achieved via the examination of the percentage of the explained variance, the shape of residuals, and the split-half analysis.[16]

3. RESULTS AND DISCUSSION

3.1. Fluorescence EEM of Individual Standards. The main ingredients of cannabis, including THC, CBN, CBD, and THC−COOH, exhibit diverse fluorescence characteristics owing to their conjugate structures (Figure 2). The fluorescence characteristics of the fluorescence maxima of the standards in methanol, including spectral position ($\lambda_{ex}/\lambda_{em}$), Stokes shift ($\lambda_{em}\lambda_{ex}$), and linear regression parameters between the fluorescence peak intensity and standards concentration, are summarized in Table 1.

THC exhibits a fluorescence peak around $\lambda_{ex}/\lambda_{em}$ = 255/310 nm, and the excitation wavelength at 290 nm exhibits an emission peak at 310 nm. As shown in Figure 3, the concentration of THC demonstrates a positive linear relationship with fluorescence peak intensity at the nanogram level (n = 5, $p < 0.01$). Compared with THC, THC−COOH exhibits a weaker peak around $\lambda_{ex}/\lambda_{em}$ = 265/285 nm because of the electron-withdrawing group of the carboxyl group on the benzene ring. A good positive linear relationship between the concentration of THC−COOH and the fluorescence intensity over the range of 0.1−1.0 μg/mL (n = 5; $p < 0.01$.) is observed. The fluorescence characteristic of CBD is similar to THC. CBD with the lowest λ_{ex} value, among these compounds, displays a strong peak around $\lambda_{ex}/\lambda_{em}$ = 235/300 nm. The concentration of CBD (Figure 3) demonstrates a good positive linear relationship with the fluorescence intensity over the range of 0.06−0.9 μg/mL (n = 5, $p < 0.01$). CBN with rich electronic properties exhibits two strong peaks around $\lambda_{ex}/\lambda_{em}$ = 255/310 and 310/360 nm. The result indicates a good positive linear relationship between the concentration of CBN and fluorescence intensity at 0.06−1.5 μg/mL. When the concentration of CBN is ≥ 2.0 μg/mL, the fluorescence peak intensity decreases with an increase in the CBN concentration probably because of the self-quenching effect, and the concentration of CBN has a nonlinear relationship with the fluorescence peak intensity. As mentioned above, the fluorescence signatures of these four psychoactive ingredients of cannabis are mainly influenced by their conjugated π-electron systems. The increase in the number of conjugated π-electrons in a fluorophore causes expend of intrinsic fluorescence capacity by increasing the molar absorption coefficient and fluorescence quantum yield.

In addition, the polarity of the solvent considerably affected the fluorescence spectra of the main psychoactive ingredients of cannabis. The methanol solvent possesses a stronger ability to dissolve THC, CBD, CBN, and THC−COOH, which is important for the fluorescence quantum yield. The high polarity and relatively weak dissolving capacity of ultrapure water decreased the fluorescence quantum yield due to changes in the nonradiative decay rate or the conformational structure of the fluorophore. The fluorescence maxima of the four compounds were stronger and more sensitive in the methanol solvent compared to that in ultrapure water, which can help obtain better linear regression parameters between the contaminant concentration and fluorescence peak intensity, including detection limit (DL) and quantification limit (QL).

3.2. Discrimination of Fluorescence Signatures in Mixtures. Herein, the compositions of the calibration and prediction samples were set based on the statistical results of the primary ingredients of cannabis in urine.[17] The complex

https://doi.org/10.1021/acsomega.3c04913
ACS Omega 2023, 8, 36302−36310

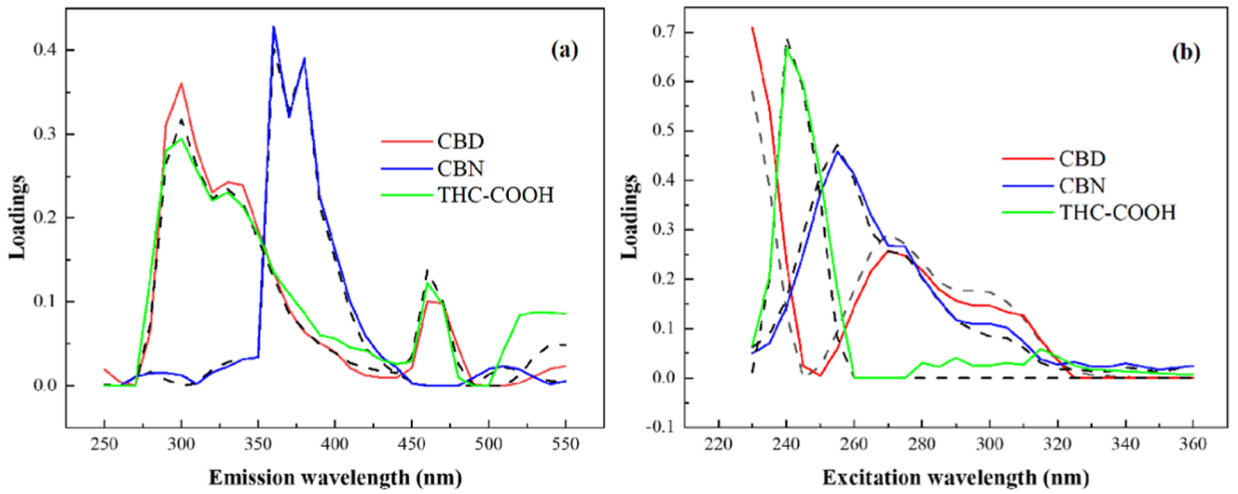

Figure 4. Comparison of emission spectra (a) and excitation spectra (b) between that validated by the three-component model (solid line) and that obtained from the EEM measurements of individual compounds (black dotted line).

samples were divided into two groups: mixture 1, which included three components (CBD, CBN, and THC−COOH) and mixture 2, which included four components (THC, CBD, CBN, and THC−COOH). For each mixture type, 25 calibration samples and 10 predicted samples were designed herein, and their EEM data sets were processed using the PARAFAC algorithm. The data of mixtures 1 and 2 are listed in Table 2 and for other samples, refer to the Supporting Information.

The components in the PARAFAC model represented the number of fluorophores in the mixture after the inner-filter effect correction.[18] The number of components in the PARAFAC model should be determined for application of the PARAFAC algorithm. Core consistency diagnostics in combination with other model parameters, such as residuals, loadings, and split-half analysis, were used to determine the number of components to avoid overestimation or underestimation for the PARAFAC model herein. The results of the PARAFAC models indicated that a four-component PARAFAC model was present in mixture 2, and a three-component PARAFAC model was selected in mixture 1. Based on the results obtained from the PARAFAC models, the true and estimated models can coincide when the appropriate number of components is considered.

Mixture 1 validated a three-component model, which included CBD, CBN, and THC−COOH fluorophores. These three compounds were identified from mixture 1 using the PARAFAC model. The excitation and emission spectra of these compounds in the mixtures validated by the PARAFAC models are consistent with those of the individual compounds obtained from the EEM measurements (Figure 4). The best overlap between the measured and modeled spectra was observed for CBN among the compounds. As previously mentioned, the $\lambda_{ex}/\lambda_{em}$ values of these psychoactive ingredients of cannabis were quite different in their three-dimensional fluorescence spectra. Hence, the PARAFAC analysis helped easily separate these compounds from the mixtures of psychoactive ingredients of cannabis.

Mixture 2 validated a four-component model, which included THC, CBD, CBN, and THC−COOH fluorophores. To identify these fluorophores, the Ex and Em spectra of the components resolved from the PARAFAC algorithm were compared to the corresponding actual spectra of individual compounds obtained from the EEM measurements, respectively. As shown in Figure 5, the comparison results indicate that PARAFAC can identify the four compounds in mixture 2 and exhibit a good correspondence between the actual spectral profiles and loadings based on the decomposition of the EEM data array. In particular, the loading scores and peak locations of the modeled spectra are identical to those of the measured spectra. Despite the presence of the compound with higher fluorescence intensity as potential interference, PARAFAC can generate a good predictive model for all of the analytes. The $\lambda_{ex}/\lambda_{em}$ values of THC and CBN are 255/310 nm; however, $\lambda_{ex}/\lambda_{em}$ values of CBN are 310/360 nm. Therefore, CBN and THC can be validated using the PARAFAC method in the mixtures.

With regard to the EEM/PARAFAC quantification of the four primary ingredients of cannabis in the mixture samples, the concentrations of the four compounds were calculated by using linear regression parameters between the individual compound concentrations and their corresponding resolved concentration scores. Representative prediction results are shown in Figure 6, and the regression between the nominal and predicted values related to the samples is shown in Figure 7. Regardless of the actual amount of these psychoactive ingredients in the solutions, PARAFAC models correctly calculated the concentrations of the compounds. In addition, Table 3, which includes statistical parameters, such as limit of quantitation (LOQ), root-mean-square error of prediction (RMSEP), and average recovery (AR suggested), indicates the good performance of the proposed PARAFAC model with regard to the determination of the main psychoactive ingredients of cannabis. Moreover, the predicted concentrations of PARAFAC could be as low as the nanogram level.

For CBN, in the low-concentration group, the mean concentrations resolved using the three-component model (64.5 ± 4.8 and 84.3 ± 5.7 ng/mL) are almost identical to the corresponding actual concentrations (65 and 85 ng/mL). Similar modeled results are observed in the four-component model, and the modeled concentrations of CBN (70.3 ± 3.3 and 90.3 ± 5.5 ng/mL) are close to the corresponding actual concentrations (70 and 88 ng/mL). The prediction results of CBD in the high concentration group were similar to those in the low-concentration group regardless of the component number of the PARAFAC model. For THC−COOH, the

https://doi.org/10.1021/acsomega.3c04913
ACS Omega 2023, 8, 36302−36310

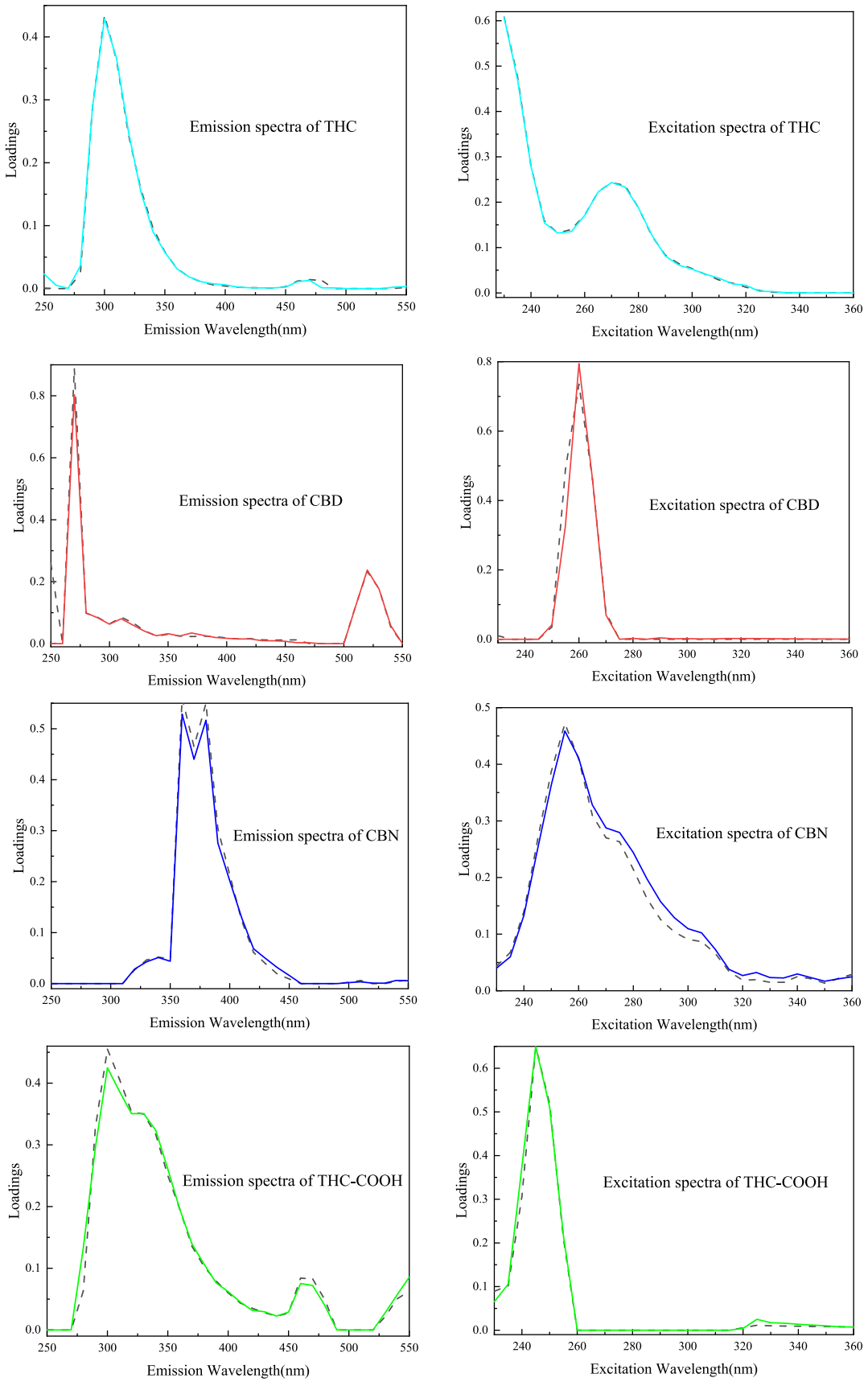

Figure 5. Loadings were validated using the PARAFAC models (dotted line) and the actual spectra obtained from the individual compounds (solid line).

https://doi.org/10.1021/acsomega.3c04913
ACS Omega 2023, 8, 36302−36310

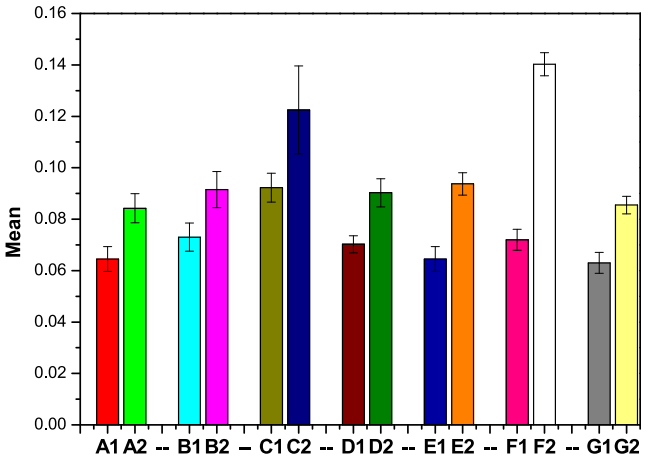

Figure 6. Prediction results of the low concentrations of the prediction samples (nos. 17, 18, 23, and 24 μg/mL) resolved using the PARAFAC method. A1 and A2: CBN in mixture 1 (nos. 17 and 18), B1 and B2: CBD in mixture 1 (nos. 17 and 18), C1 and C2: THC−COOH in mixture 1 (nos. 17 and 18); D1 and D2: CBN in mixture 2 (nos. 23 and 24), E1 and E2: CBD in mixture 2 (nos. 23 and 24), F1 and F2: THC−COOH in mixture 2 (nos. 23 and 24), and G1 and G2: THC in mixture 2 (nos. 23 and 24).

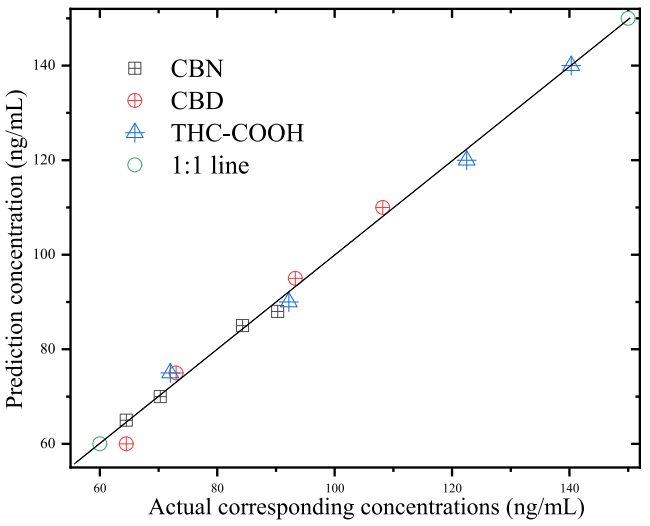

Figure 7. Predicted concentrations decomposed using the PARAFAC method and actual concentrations for CBN, CBD, and THC−COOH.

modeled results of PARAFAC can fit with the actual concentrations but with a large standard deviation. In the low-concentration group, the mean concentrations of THC−COOH resolved from the three-component model (92.2 ± 5.6 and 122.5 ± 17.1 ng/mL) are relatively close to the real corresponding concentrations (90 and 120 ng/mL), and the standard deviation of THC−COOH is larger than that of other psychoactive ingredients. However, the prediction concentrations of THC−COOH resolved from the four-component model are 72.0 ± 4.1 and 140.3 ± 4.5 ng/mL, respectively (the actual corresponding concentrations are 75 and 140 ng/mL), which is much better than that from the three-component model. In the high-concentration group, the prediction results of THC−COOH were similar to those in the low-concentration group. For THC, the PARAFAC-based four-component model can correctly calculate the concentrations in prediction samples, and the mean concentrations of THC derived from PARAFAC analysis are close to their true corresponding concentrations with small standard deviations in mixture 2. Consequently, these results indicate that the EEM/PARAFAC identification and quantification of psychoactive ingredients of cannabis are efficient at the nanogram level, which might be applied to the analysis of cannabis in urine.

3.3. Application to Urine Samples. Two urine samples donated by frequent cannabis users and two reference urine samples were artificially added to the main ingredients of cannabis to test the EEM/PARAFAC method using the blind test. At the same time, GC−MS was used as a control test to analyze these samples. The experimental results (Figure 8) indicate that there are good correlations between the EEM/PARAFAC method and GC−MS with a low RMSEP range of 0.01−0.05 μg/mL and a good LOQ range of 0.07−0.44 μg/mL (Supporting Information). The methods could not detect THC in urine samples due to a minor amount after the metabolic process. However, the PARAFAC algorithm helped determine THC in the reference urine samples compared to the results of GC−MS. The mean value (65 ± 4.4 ng/mL) obtained using PARAFAC was very close to the results of GC−MS (68 ng/mL), which indicates that the EEM/

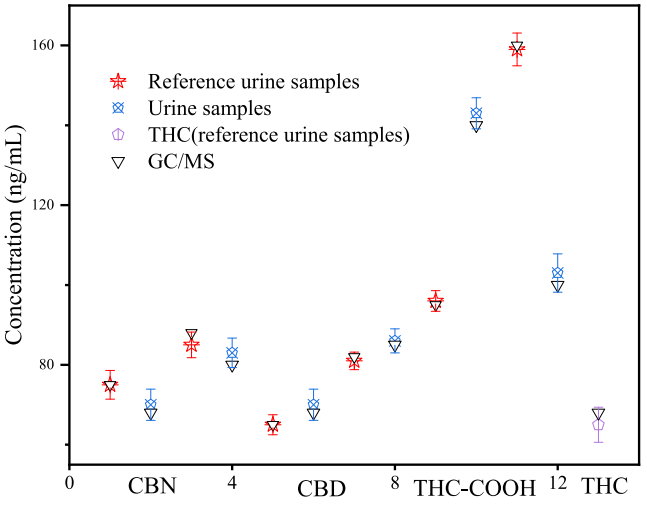

Figure 8. Concentrations of the main psychoactive ingredients of cannabis in the urine samples (ng/mL) from the EEM/PARAFAC method and GC−MS analysis, $n = 5$, $p < 0.01$.

Table 3. Statistic Parameters Obtained from the PARAFAC Model (Calibration and Prediction Samples)

	mixture 1			mixture 2			
statistic parameters	CBD	CBN	THC−COOH	CBD	CBN	THC−COOH	THC
AR (%)	103 ± 4.2	99 ± 5.5	106 ± 3.6	104 ± 5.2	99 ± 6.1	95 ± 3.7	107 ± 2.9
RMSEP (μg/mL)	0.005	0.003	0.014	0.027	0.020	0.053	0.070
LOQ (μg/mL)	0.46	0.48	0.32	0.71	0.32	0.43	0.26

https://doi.org/10.1021/acsomega.3c04913
ACS Omega 2023, 8, 36302−36310

PARAFAC method can be applied to various extracts of cannabis. The prediction results of CBD and CBN decomposed by the PARAFAC model agree well with the analysis results of GC−MS. The relative errors of the mean values of CBD and CBN were obtained from the PARAFAC range of −2.3 to 2.9%, and the standard deviations of these mean values ranged from 2.2 to 3.9. The good correlations between these two techniques implied that the EEM/PARAFAC method could substitute chromatographic analysis for CBD and CBN in urine. The identification and quantification of THC−COOH, among the main psychoactive ingredients of cannabis, in urine are being mainly considered, which is the analytics target in the cases of cannabis abuse in China. The EEM/PARAFAC method can accurately obtain the concentrations of THC−COOH in both urine samples and reference urine samples. The mean values obtained from PARAFAC analysis are very close to the results of GC−MS with small standard deviations.

4. CONCLUSIONS

Herein, the EEM coupled with the PARAFAC method was developed to identify and quantify the four main psychoactive ingredients of cannabis in urine samples at the ng/mL level, and the prediction ability of the models was validated by comparing results with those obtained from the parallel GC−MS analysis. Moreover, the fluorescence characteristics of THC, THC−COOH, CBN, and CBD were investigated. Fluorescence results suggested that the four main psychoactive ingredients of cannabis, including THC, THC−COOH, CBN, and CBD, exhibited strong fluorescence intensity due to their conjugate structures and different fluorescence characteristics at the ng/mL level. The concentrations of the main psychoactive ingredients of cannabis exhibited a good positive linear relationship with the fluorescence intensity. Both of them are the basis of qualitative and quantitative analyses using EEM coupled with the PARAFAC method. The study results indicated that the mean values obtained by EEM/PARAFAC correlated well with the results of GC−MS in the urine samples of abusers and reference urine samples with small standard deviations. The EEM spectroscopic investigation coupled with the PARAFAC algorithm helped provide an organic, solvent-less, fast, reliable tool to perform the accurate timely screening of cannabis abusers.

■ ASSOCIATED CONTENT

Supporting Information

The Supporting Information is available free of charge at https://pubs.acs.org/doi/10.1021/acsomega.3c04913.

EEM of samples (PDF)

■ AUTHOR INFORMATION

Corresponding Author

Sheng-Feng Cui − *Center for Traffic Evidence Technology, Department of Criminal Science and Technology, Railway Police College, Zhengzhou 450053, China; Institute of Public Safety, Zhengzhou University, Zhengzhou 450001, China;* orcid.org/0009-0004-8120-4669; Phone: +86-371-60666173; Email: cuishengfeng@rpc.edu.cn; Fax: +86-371-60666173

Authors

Hai-Long Yang − *Center for Traffic Evidence Technology, Department of Criminal Science and Technology, Railway Police College, Zhengzhou 450053, China*

Si-Yu Lin − *Center for Traffic Evidence Technology, Department of Criminal Science and Technology, Railway Police College, Zhengzhou 450053, China*

Jing-Wei Wan − *Center for Traffic Evidence Technology, Department of Criminal Science and Technology, Railway Police College, Zhengzhou 450053, China; Institute of Public Safety, Zhengzhou University, Zhengzhou 450001, China*

Cheng-He Zhou − *Key Laboratory of Applied Chemistry of Chongqing Municipality, School of Chemistry and Chemical Engineering, Southwest University, Chongqing 400715, China;* orcid.org/0000-0003-3233-5465

Complete contact information is available at: https://pubs.acs.org/10.1021/acsomega.3c04913

Author Contributions

Experimental data were obtained by Si-Yu Lin and Hai-Long Yang. Dr. Cheng-He Zhou and Dr Jing-Wei Wan contributed to the overall design of the experiments and interpretation of the data. Dr. Sheng-Feng Cui conceived the study and contributed to the design, acquisition and interpretation of the data, and wrote drafts of the manuscript. All authors approved the final version of the manuscript.

Notes

The authors declare no competing financial interest.

■ ACKNOWLEDGMENTS

This research was partially supported by the National Natural Science Foundation of China (NSFC) (no. 21805208), the Henan Scientific and Technological Research Projects (212102310487), and the Research Funds for the Central Universities (2019TJJBKY032 and 2020TJJBKY005).

■ REFERENCES

(1) Withey, S. L.; Bergman, J.; Huestis, M. A.; George, S. R.; Madras, B. K. THC and CBD blood and brain concentrations following daily administration to adolescent primates. *Drug Alcohol Depend.* **2020**, *213*, 108129−108136.

(2) Peacock, A.; Leung, J.; Larney, S.; Colledge, S.; Hickman, M.; Rehm, J.; Giovino, G. A.; West, R.; Hall, W.; Griffiths, P.; Ali, R.; Gowing, L.; Marsden, J.; Ferrari, A. J.; Grebely, J.; Farrell, M.; Degenhardt, L. Global statistics on alcohol, tobacco and illicit drug use: 2017 status report. *Addiction* **2018**, *113*, 1905−1926.

(3) Hanuš, L. O.; Meyer, S. M.; Muñoz, E.; Taglialatela-Scafati, O.; Appendino, G. Phytocannabinoids: a unified critical inventory. *Nat. Prod. Rep.* **2016**, *33*, 1357−1392.

(4) D'Elia, V.; Montalvo, G.; Ruiz, C. G.; Ermolenkov, V. V.; Ahmed, Y.; Lednev, I. K. Ultraviolet resonance Raman spectroscopy for the detection of cocaine in oral fluid. *Spectrochim. Acta Mol. Biomol. Spectrosc.* **2018**, *188*, 338−340.

(5) Dubrow, G. A.; Pawar, R. S.; Srigley, C.; Fong Sam, J.; Talavera, C.; Parker, C. H.; Noonan, G. O. A survey of cannabinoids and toxic elements in hemp-derived products from the United States marketplace. *J. Food Compos. Anal.* **2021**, *97*, 103800−103809.

(6) Risoluti, R.; Gullifa, G.; Battistini, A.; Materazzi, S. MicroNIR/Chemometrics: A new analytical platform for fast and accurate detection of Δ9-Tetrahydrocannabinol (THC) in oral fluids. *Drug Alcohol Depend.* **2019**, *205*, 107578.

(7) Moreira, L. P.; Silveira, L.; Pacheco, M. T. T.; da Silva, A. G.; Rocco, D. D. F. M. Detecting urine metabolites related to training performance in swimming athletes by means of Raman spectroscopy

and principal component analysis. *J. Photochem. Photobiol., B* **2018**, *185*, 223−234.
(8) Yan, M.; Fu, Q.; Li, D.; Gao, G.; Wang, D. Study of the pH influence on the optical properties of dissolved organic matter using fluorescence excitation-emission matrix and parallel factor analysis. *J. Lumin.* **2013**, *142*, 103−109.
(9) Akbarian, S.; Kompany-Zareh, M.; Najafpour, M. M.; Tomo, T.; Allakhverdiev, S. I. Unsupervised classification of PSII with and without water-oxidizing complex samples by PARAFAC resolution of excitation-emission fluorescence images. *J. Photochem. Photobiol., B* **2019**, *195*, 58−66.
(10) Ferretto, N.; Tedetti, M.; Guigue, C.; Mounier, S.; Redon, R.; Goutx, M. Identification and quantification of known polycyclic aromatic hydrocarbons and pesticides in complex mixtures using fluorescence excitation-emission matrices and parallel factor analysis. *Chemosphere* **2014**, *107*, 344−353.
(11) Xu, B.; Ye, Y.; Liao, L. Rapid and simple analysis of amphetamine-type illegal drugs using excitation-emission matrix fluorescence coupled with parallel factor analysis. *Forensic Sci. Res.* **2019**, *4*, 179−187.
(12) Cui, S. F.; Addla, D.; Zhou, C. H. Novel 3-amino-thiazolquinolones: Design, synthesis, bioactive evaluation, SARs, and preliminary antibacterial mechanism. *J. Med. Chem.* **2016**, *59*, 4488−4510.
(13) Cui, S. F.; Wan, J. W.; Zhou, C. H. Fluorescence spectroscopic analysis on the synergistic mechanism of diazepam and ethanol. *Chem. J. Chin. Univ.* **2018**, *39*, 1178−1184.
(14) Cui, S. F.; Li, W.; Zhou, C. H. Molecular spectroscopic studies examining the interactions between phenobarbital and human serum albumin in alcohol consumption. *Am. J. Drug Alcohol Abuse* **2018**, *44*, 321−328.
(15) Baghoth, S. A.; Sharma, S. K.; Amy, G. L. Tracking natural organic matter (NOM) in a drinking water treatment plant using fluorescence excitation emission matrices and PARAFAC. *Water Res.* **2011**, *45*, 797−809.
(16) Kamstrup-Nielsen, M. H.; Johnsen, L. G.; Bro, R. Core consistency diagnostic in PARAFAC2. *J. Chemom.* **2013**, *27*, 99−105.
(17) Desrosiers, N. A.; Lee, D.; Scheidweiler, K. B.; Concheiro-Guisan, M.; Gorelick, D. A.; Huestis, M. A. In vitro stability of free and glucuronidated cannabinoids in urine following controlled smoked cannabis. *Anal. Bioanal. Chem.* **2014**, *406*, 785−792.
(18) Stedmon, C. A.; Bro, R. Characterizing dissolved organic matter fluorescence with parallel factor analysis: a tutorial. *Limnol Oceanogr. Methods* **2008**, *6*, 572−579.

https://doi.org/10.1021/acsomega.3c04913
ACS Omega 2023, 8, 36302−36310